Hybrid Calcium Phosphate-Polymeric Micelles Incorporating Gadolinium Chelates for Imaging-Guided Gadolinium Neutron Capture Tumor Therapy

Peng Mi,[†,‡,§] Novriana Dewi,[⊥] Hironobu Yanagie,[⊥] Daisuke Kokuryo,[∥] Minoru Suzuki,[#] Yoshinori Sakurai,[#] Yanmin Li,[▽] Ichio Aoki,[∥] Koji Ono,[#] Hiroyuki Takahashi,[⊥] Horacio Cabral,[▽] Nobuhiro Nishiyama,[*,†,‡] and Kazunori Kataoka[*,†,§,▽,⊗]

[†]Innovation Center of Nanomedicine, Kawasaki Institute of Industry Promotion, 66-20 Horikawa-cho, Saiwai-ku, Kawasaki 212-0013, Japan, [‡]Polymer Chemistry Division, Chemical Resources Laboratory, Tokyo Institute of Technology, R1-11, 4259 Nagatsuta, Midori-ku, Yokohama 226-8503, Japan, [§]Center for Disease Biology and Integrative Medicine, Graduate School of Medicine, The University of Tokyo, 7-3-1 Hongo, Bunkyo-ku, Tokyo 113-8656, Japan, [⊥]Department of Nuclear Engineering and Management, Graduate School of Engineering, The University of Tokyo, 7-3-1 Hongo, Bunkyo-ku, Tokyo 113-8656, Japan, [∥]Molecular Imaging Center, National Institute of Radiological Sciences, Anagawa 4-9-1, Inage, Chiba, 263-8555, Japan, [#]Research Reactor Institute, Kyoto University, Asahiro nishi, Kumatori-cho, Sennan-gun, Osaka 590-0494, Japan, [▽]Department of Bioengineering, Graduate School of Engineering, The University of Tokyo, 7-3-1 Hongo, Bunkyo-ku, Tokyo 113-8656, Japan, and [⊗]Department of Materials Engineering, Graduate School of Engineering, The University of Tokyo, 7-3-1 Hongo, Bunkyo-ku, Tokyo 113-8656, Japan

ABSTRACT Gadolinium (Gd) chelates-loaded nanocarriers have high potential for achieving magnetic resonance imaging (MRI)-guided Gd neutron capture therapy (GdNCT) of tumors. Herein, we developed calcium phosphate micelles hybridized with PEG-polyanion block copolymers, and incorporated with the clinical MRI contrast agent Gd-diethylenetriaminepentaacetic acid (Gd-DTPA/CaP). The Gd-DTPA/CaP were nontoxic to cancer cells at the concentration of 100 μM based on Gd-DTPA, while over 50% of the cancer cells were killed by thermal neutron irradiation at this concentration. Moreover, the Gd-DTPA/CaP showed a dramatically increased accumulation of Gd-DTPA in tumors, leading to the selective contrast enhancement of tumor tissues for precise tumor location by MRI. The enhanced tumor-to-blood distribution ratio of Gd-DTPA/CaP resulted in the effective suppression of tumor growth without loss of body weight, indicating the potential of Gd-DTPA/CaP for safe cancer treatment.

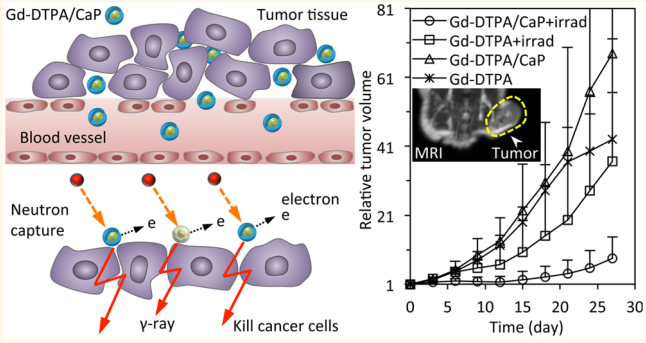

KEYWORDS: gadolinium neutron capture therapy · calcium phosphate micelle · drug delivery system · MRI

Neutron capture therapy (NCT) is a binary therapeutic modality for tumor treatment, demonstrating high clinical performance with extended survival periods.[1,2] The damage of NCT to cancer cells is mediated by radiations emitted from nonradioactive NCT agents upon capturing thermal neutrons, while the low energy of the thermal neutron irradiation does not cause damage to normal organs without NCT agents.[3,4] Thus, providing sufficient cell-killing irradiation in the tumor regions while avoiding normal tissues is quite critical for NCT. One requirement is that only the regions of tumor tissues would be irradiated by thermal neutrons, which requires precise location of the neoplastic regions. The imaging-guided thermal neutron irradiation would facilitate the NCT of tumors, as some clinical imaging modalities such as MRI can precisely detect tumors with high resolution at micrometer scale.[5,6] Another requirement is that the NCT agents should specifically accumulate in tumor tissues while avoiding normal tissues or organs.

Chemical agents containing ^{6}Li, ^{10}B, ^{157}Gd, or ^{235}U nuclides have exhibited the

* Address correspondence to nishiyama@res.titech.ac.jp, kataoka@bmw.t.u-tokyo.ac.jp.

Received for review January 24, 2015 and accepted June 1, 2015.

Published online June 01, 2015
10.1021/acsnano.5b00532

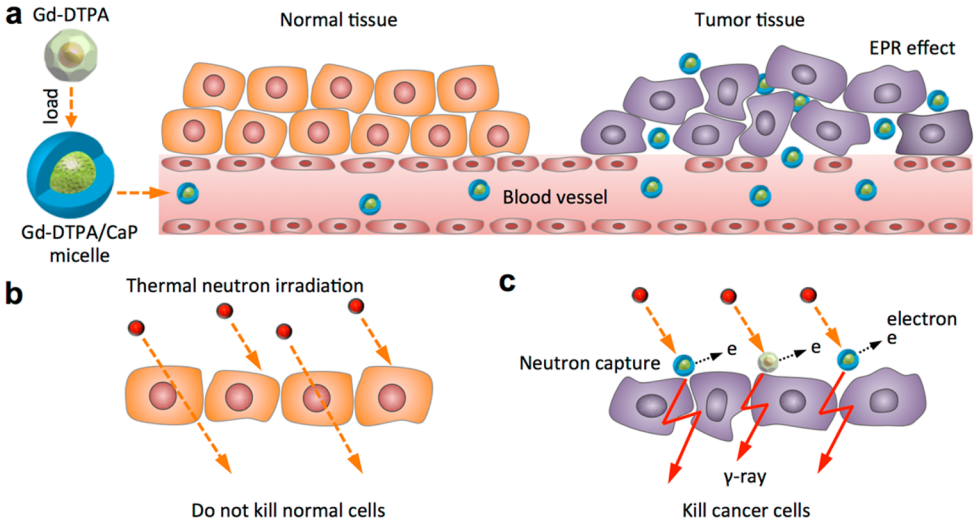

Figure 1. Scheme of Gd-DTPA/CaP hybrid micelles targeting tumors for gadolinium neutron capture therapy (GdNCT). (a) The accumulation of Gd-DTPA delivered by Gd-DTPA/CaP in tumors through the EPR effect. (b) Low energy thermal neutron irradiation does not kill normal cells without NCT agents. (c) Thermal neutron irradiation could kill or cause hazardous damage to cancer cells by the γ-rays emitted from the Gd nuclides after nuclear reaction with captured thermal neutrons.

ability for NCT, and several ^{10}B-based agents have been approved for clinical application.[7] Among those agents, the gadolinium (^{157}Gd) nuclide has the largest capture cross-section of 255 000 barns for thermal neutron absorption (over 66 times larger than that of ^{10}B) and emits γ-rays with a high energy of 7.8 MeV in the neutron capture reaction associated with electrons of low energy.[8] The high-energy γ-rays from ^{157}Gd have a long radiation range that can damage tumor cells across whole tumor tissues to suppress the tumor growth, which is beyond the range of the secondary particles, short-range disintegration products emitted from the ^{10}B nuclides in boron neutron capture therapy (BNCT).[9] Meanwhile, the Auger electrons may further enhance the therapeutic effects, as some reports indicated that partially chelated Gd(III) could access the nuclei of cancer cells and break the double-strand of DNA by thermal neutron irradiation.[10,11] Moreover, the paramagnetic Gd(III) chelates, such as Gd-DTPA and Gd-tetraazacyclododecane tetraacetic acid (Gd-DOTA), can enhance the T_1-weighted contrast for MRI because the unpaired electrons of the Gd ions (Gd^{3+}) exhibit strong water proton spin−lattice relaxation effect,[12] which could be exploited to delineate the outline and location of tumors for MR imaging-guided GdNCT, while other types of NCT agents lack such diagnostic function. However, the fast clearance and systemic distribution of low-molecular-weight Gd(III) chelates hinder the targeting of tumor tissues with effective doses for diagnosis and NCT. Moreover, the systemic distribution of the Gd(III) chelates may induce unnecessary exposure of healthy tissues to γ-rays or ionizing irradiation. Thus, Gd-based NCT agents should be delivered specifically to tumor tissues, and nanocarriers have been studied for their application in tumor-specific drug delivery.[6,13−19]

Several nanocarriers have demonstrated their utility in neutron capture therapy,[7,20−25] though most of them do not present the imaging-guided NCT function that can facilitate the precise irradiation of entire tumor tissues while avoiding normal regions. Thus, there is a demand for rationally designed nanocarriers for delivering Gd-based NCT agents to tumor tissues with high tumor-to-blood ratio to achieve effective tumor treatment based on precise imaging-guided thermal neutron irradiation. Herein, we applied biocompatible calcium phosphate (CaP) micelles incorporating Gd-DTPA (Gd-DTPA/CaP) for dual MR cancer imaging and tumor ablation by GdNCT. After intravenous administration, the sub-100 nm Gd-DTPA/CaP accumulated in the tumor tissues as a result of the enhanced permeability and retention (EPR) effect,[26] while avoiding systemic distribution in normal tissues (Figure 1a). After thermal neutron irradiation, the Gd atoms in the tumors captured the thermal neutrons and emitted γ-rays of high energy, thus suppressing tumor growth while avoiding damage to healthy tissues that without distribution of NCT agents (Figure 1b,c).

RESULTS AND DISCUSSION

Characterization of Gd-DTPA/CaP. Monodispersed Gd-DTPA/CaP, with number-average diameter of approximately 55 nm and polydispersity index (PDI) of approximately 0.1 (Figure 2a), were obtained by hybridizing PEG-poly(aspartic acid) (PEG−PAsp) block copolymers because the carboxylic groups of PAsp could interact with Ca^{2+} for size control. In this formulation, the PAsp segments can avoid the formation of big hydroxyapatite (HA) crystals inside the core, while the PEG segments could prevent further growth of the CaP core,[27−29] leading to controllable particle

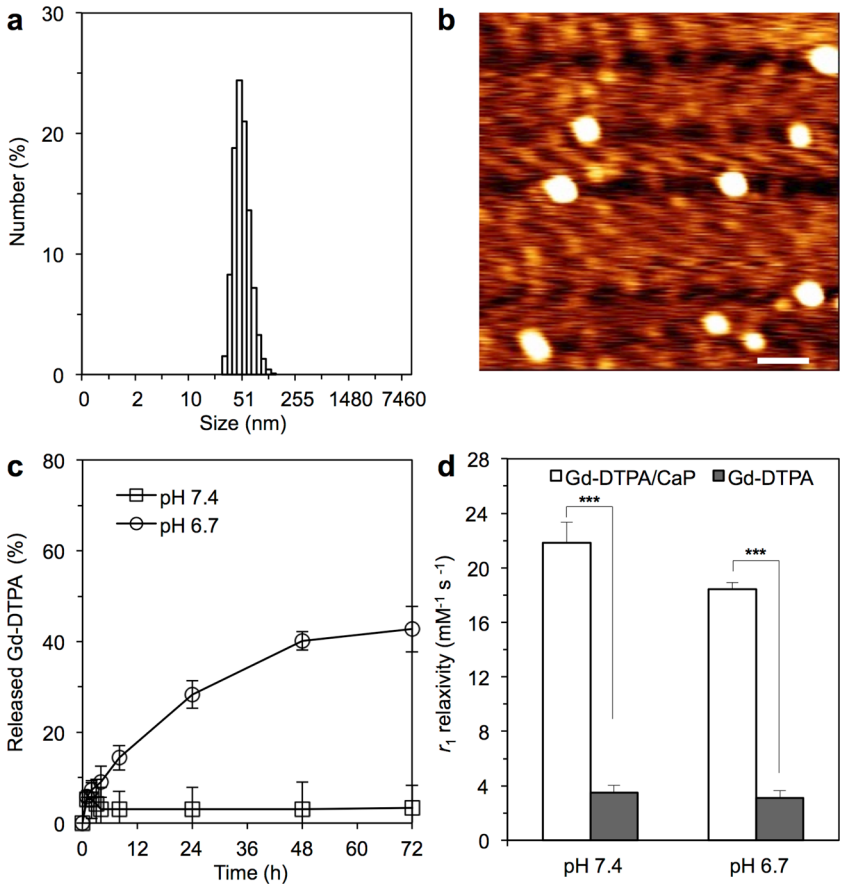

Figure 2. Characterization of Gd-DTPA/CaP hybrid micelles. (a) Number-average diameter of Gd-DTPA/CaP measured by DLS. (b) Morphology of Gd-DTPA/CaP characterized by AFM, scale bar 50 nm. (c) Release profile of Gd-DTPA/CaP in DMEM containing 10% FBS at pH 7.4 and pH 6.7 at 37 °C to mimic the conditions of the bloodstream and tumor tissues, respectively. (d) The r_1 relaxivity of Gd-DTPA/CaP in 10 mM PBS buffer containing 150 mM NaCl at pH 7.4 and pH 6.7 at 37 °C. The data are expressed as the mean ± SD, ***$p < 0.001$ compared to Gd-DTPA.

size in the sub-100 nm range. Atomic force microscopy (AFM) also revealed the formation of monodispersed Gd-DTPA/CaP without agglomeration (Figure 2b). Then, the release rates of Gd-DTPA from the Gd-DTPA/CaP micelles were evaluated in Dulbecco's modified Eagle medium (DMEM) at pH 6.7 and 37 °C with shaking to simulate the pH conditions of tumor tissues.[30] Accordingly, 42% of Gd-DTPA was released from the Gd-DTPA/CaP micelles at pH 6.7 because of the partial dissolution of the CaP materials in acidic buffers,[31] whereas only 5% was released at pH 7.4 within 72 h (Figure 2c). These values indicate that Gd-DTPA/CaP is stable in the normal pH environment of blood circulation (pH 7.4), which appropriately correlates with the previously reported dissociation kinetics and stability conformation of polymeric CaP micelles.[32,33] The longitudinal relaxation rate r_1, which reflects the enhancement of the water proton relaxation rate (T_1^{-1}), was also measured after incubation at pH 7.4 or 6.7 for 4 h. The Gd-DTPA/CaP exhibited a much higher molecular relaxivity (18.4 mM^{-1} s^{-1}) than Gd-DTPA (3.1 mM^{-1} s^{-1}) at both pH 7.4 and 6.7 ($p < 0.001$) (Figure 2d). Such an increase in the molecular relaxivity may be due to the confinement of Gd-DTPA inside the core of the CaP micelles, which may decrease the water exchange rate between bulk water and inner-sphere water,[34] and slow down the tumbling motion (τ_R) of Gd-DTPA.[35] Thus, the relaxivity of Gd-DTPA/CaP was slightly lower after incubation at pH 6.7 for 4 h, probably due to the partial release of Gd-DTPA (9%) at this pH.

Cell Viability after Neutron Irradiation with Gd-DTPA/CaP. The cellular viability was evaluated to test the potential of Gd-DTPA/CaP as an effective NCT agent. Thus, murine colon adenocarcinoma (C26) cells were exposed to Gd-DTPA/CaP for 24 h and then exposed to thermal neutron irradiation at a dose of $1.6-2.2 \times 10^{12}$ neutron/cm^2 for 1 h at the Gd-DTPA-based concentration of 100 μM, which is nontoxic to C26 cancer cells without thermal neutron irradiation. Thereafter, the cell viability was measured 24 h after irradiation. The results demonstrated that the survival rate of the C26 cancer cells significantly decreased after thermal neutron irradiation, and fewer than 50% of the cancer cells survived in both the Gd-DTPA/CaP and Gd-DTPA groups; however, there was no cytotoxicity at the same dose without irradiation (Figure 3). Thus, Gd-DTPA/CaP could successfully attack cancer cells by emitting

γ-rays and could be used as an effective NCT agent. Moreover, the Auger electrons could also attack the cancer cells by inducing double-strand breaks during the NCT,[10] as Gd-DTPA/CaP were found inside the cells in a comparable level to that of Gd-DTPA (Supporting Information Figure S1), corresponding to the levels of Gd-DTPA uptake reported in the literature.[11] It was reported that approximately 80% of the nuclei of glioblastoma multiforme (GBM) cancer cells contained Gd after exposure to Gd-DTPA for 24 h,[36] which could inhibit the further proliferation of cancer cells during NCT.

***In Vivo* Plasma Clearance and Tumor Accumulation of Gd-DTPA/CaP.** Gd-DTPA/CaP at the dose of 0.02 mmol/kg was intravenously administrated to mice bearing subcutaneous C26 tumors to evaluate their plasma clearance and tumor accumulation. Gd-DTPA/CaP exhibited a much longer retention time in plasma and organs than the low-molecular-weight Gd-DTPA chelates, which were rapidly cleared from circulation (Figure 4a and Supporting Information Figure S2−S4). Meanwhile, the amount of Gd-DTPA delivered to the tumor tissues gradually increased from 2.2% in 3 h to 3.9% in 10 h and remained constant until 24 h (Figure 4b), which can be attributed to the EPR effect-mediated accumulation of Gd-DTPA/CaP.[26] Conversely, the low-molecular-weight Gd-DTPA failed to accumulate in solid tumors. Importantly, Gd-DTPA/CaP were gradually cleared from the blood circulation within 24 h, and the associated tumor-to-blood distribution ratio indicated the preferential availability in tumor tissues than in blood 24 h after intravenous administration (Figure 4c), which could provide low Gd-DTPA/CaP levels in the blood background for thermal neutron irradiation.

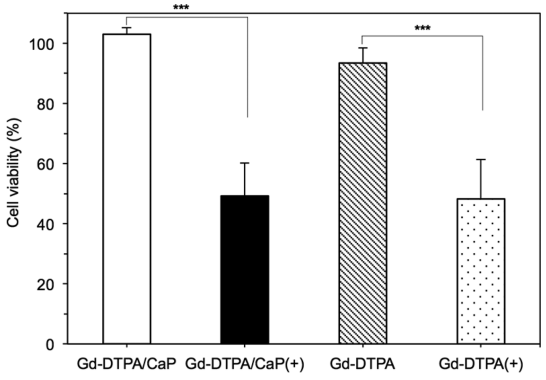

Figure 3. *In vitro* **cell viability after thermal neutron irradiation of Gd-DTPA/CaP. C26 cells were exposed to Gd-DTPA or Gd-DTPA/CaP in a Gd-DTPA basis of 100 μM for 24 h, then irradiated with thermal neutrons for 1 h, and finally, the cell viability was measured after incubation for 24 h. Nonirradiated cells exposed to Gd-DTPA/CaP at the same dose for 48 h were used as control. Gd-DTPA/CaP(+) and Gd-DTPA(+) represent the cells with thermal neutron irradiation. The data are expressed as the mean ± SD, ***$p < 0.001$ compared to the groups without thermal neutron irradiation.**

***In Vivo* MR Cancer Imaging with Gd-DTPA/CaP.** The contrast ability of Gd-DTPA/CaP was directly compared with the clinically used contrast agent Gd-DTPA. The Gd-DTPA/CaP was intravenously injected to subcutaneous C26 tumor-bearing mice, and the images were obtained with 1T MRI. After administration of Gd-DTPA/CaP, the tumor regions in mice exhibited enhanced contrast, whereas there was no contrast enhancement in mice injected with free Gd-DTPA (Figure 5a,b). After calculating the tumor-to-normal tissue (T/N) contrast intensity in both groups, the contrast in the tumor tissues was increased over 40% by Gd-DTPA/CaP with a T/N contrast ratio of 1.41, which was higher than that of Gd-DTPA, which failed to increase the contrast intensity of tumors (Figure 5c). Gd-DTPA/CaP enhanced the contrast of tumors due to their high relaxivity and the high accumulation of Gd-DTPA in the tumors through the EPR effect. The imaging results could provide accurate anatomical position of solid tumors for imaging-guided thermal neutron irradiation, especially for local thermal neutron irradiation, thereby avoiding unnecessary irradiation of normal tissues.

Gd-DTPA/CaP for Gadolinium Neutron Capture Therapy (GdNCT) of Tumors. Gd-DTPA/CaP and Gd-DTPA at 8.25 mg/kg based on Gd-compound were tested for GdNCT in subcutaneous C26 tumor-bearing mice. Twenty-four hours after intravenous injection of Gd-DTPA/CaP or Gd-DTPA, we irradiated the C26

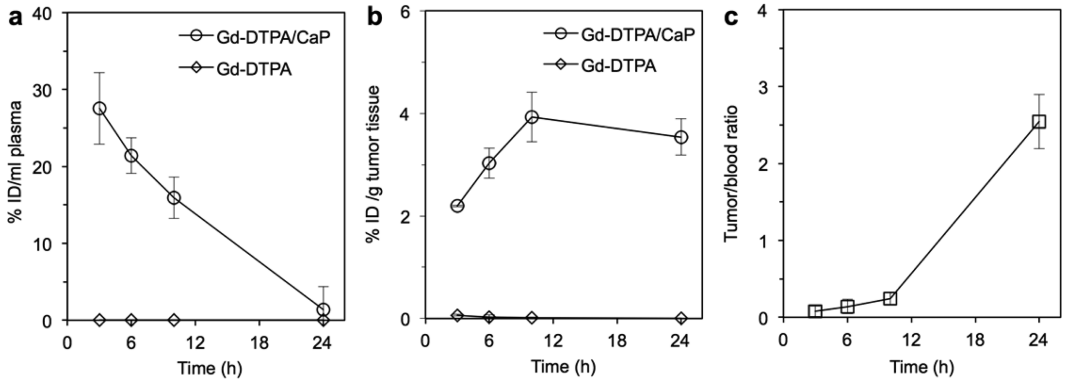

Figure 4. Plasma clearance and tumor accumulation of Gd-DTPA/CaP in mice bearing subcutaneous C26 tumors. (a) Plasma clearance of Gd-DTPA/CaP and Gd-DTPA (n = 3). (b) Tumor accumulation of Gd-DTPA/CaP (n = 3). (c) The tumor-to-blood distribution ratio at different time points after administration of Gd-DTPA/CaP. The data are expressed as the mean ± SD.

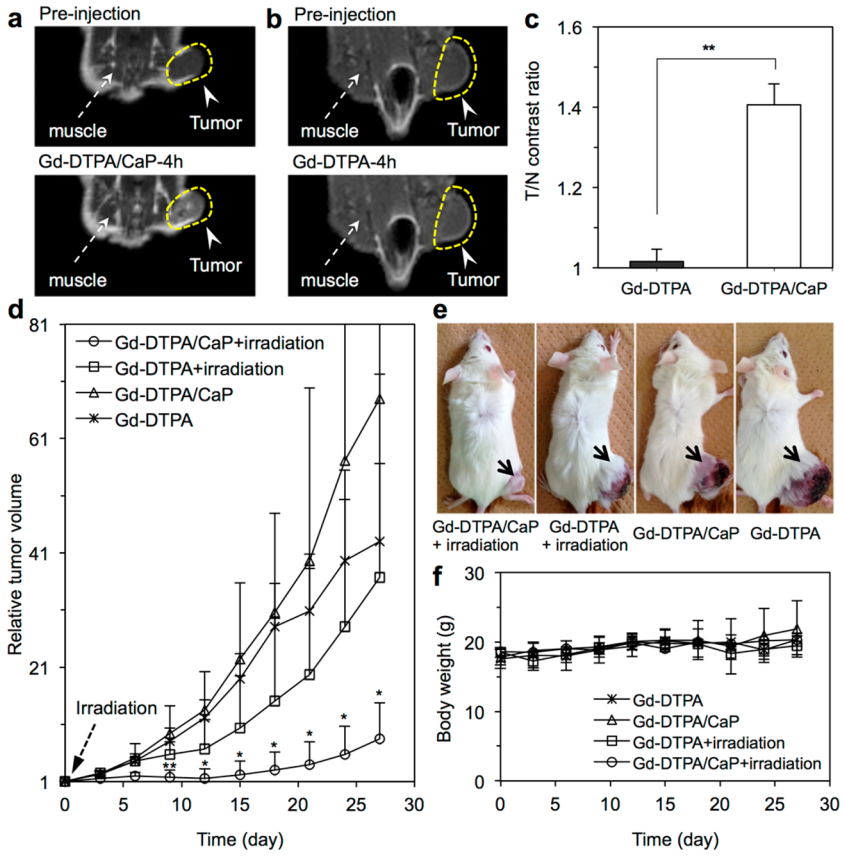

Figure 5. ***In vivo*** **MR imaging-guided neutron capture therapy with Gd-DTPA/CaP. (a,b)** ***In vivo*** **images of mice bearing subcutaneous C26 tumors after intravenous injection of Gd-DTPA/CaP (a) and Gd-DTPA (b), respectively. (c) A comparison of the tumor-to-normal tissue (T/N) contrast intensity calculated from (a) and (b) by comparing the signal intensity of the regions of interest (ROI) between tumors and normal tissues. The data are expressed as the mean ± SD (n = 3), $^{**}p < 0.01$ compared to Gd-DTPA. (d) The growth curve of the subcutaneous C26 tumors after administration of Gd-DTPA/CaP and treatment with thermal neutron irradiation for 1 h. The tumors were irradiated 24 h after the intravenous injection of Gd-DTPA/CaP (day 0). Data are expressed as the mean ± SD (n = 4 or 5), $^{**}p < 0.01$ and $^{*}p < 0.05$ compared to other groups. (e) Images of mice bearing subcutaneous C26 tumors 27 days after GdNCT. (f) Relative changes in the body weight of the mice after thermal neutron irradiation.**

tumors with a thermal neutron beam at the dose of $1.6-2.2 \times 10^{12}$ neutron/cm^2 for 1 h. Without thermal neutron irradiation, Gd-DTPA/CaP and Gd-DTPA did not affect the tumor growth rates, and the tumor volumes increased by over 40-fold at day 27 (Figure 5d). With thermal neutron irradiation, the growth rate of the tumor volume in mice injected with Gd-DTPA showed a moderate increase until day 12, but finally, the tumor reached a comparable size to that present in the mice injected with Gd-DTPA but that were not irradiated. On the other hand, when the mice injected with Gd-DTPA/CaP were exposed to thermal neutron irradiation, the C26 tumors did not grow until day 12 ($p < 0.01$) and then grew at a much slower rate than in the other control groups ($p < 0.05$). As shown in the pictures of tumors at day 27 (Figure 5e), the tumor volume with Gd-DTPA/CaP injection and neutron irradiation was much smaller than that of other groups, demonstrating that the Gd-DTPA/CaP could significantly enhance the therapeutic effects of GdNCT. The effective tumor ablation by Gd-DTPA/CaP could be associated with the high accumulation of Gd-DTPA in tumor tissues, which may capture sufficient thermal neutrons to emit γ-rays to kill a large fraction of cancer cells in tumor tissues. Besides the long-range high-energy γ-rays, and the electrons that are produced in NCT could also effectively attack tumor cells. Indeed, it has been reported that Gd compounds could access the nuclei of tumor cells[11] and enter 12% of the tumor cell nuclei in human GBM tumor tissues after a single injection of low-molecular-weight Gd-DTPA.[36] Compared to Gd-DTPA, the Gd-DTPA/CaP could deliver more Gd-DTPA to tumor tissues, which may result in more cellular uptake for a more efficient attack of tumor cells. It is also worth noting that the body weight of the mice barely changed after GdNCT (Figure 5f), suggesting the safety of Gd-DTPA/CaP for NCT.

After thermal neutron irradiation for 27 days, the tumor tissues were collected for pathological study with hematoxylin and eosin (H&E) staining. The pathological information confirmed the therapeutic effect of Gd-DTPA/CaP in GdNCT. Most cancer cells were damaged in tumor tissues treated with Gd-DTPA/CaP and thermal neutron irradiation (Figure 6b), while other samples did not show this extensive cellular damage (Figure 6a,c,d), even for tumors treated with

Gd-DTPA and thermal neutron irradiation (Figure 6d). Although most cancer cells died in the tumors injected with Gd-DTPA/CaP and submitted to thermal neutron irradiation (Figure 6b), some cancer cells still survived probably because of the presence of hypoxic tumor cells that were resistant to radiotherapy.[37]

The results obtained in this study showed that the administration of Gd-DTPA/CaP to C26 tumor-bearing mice followed by thermal neutron irradiation resulted in the effective suppression of tumor growth (Figure 5), which was not the case with the administration of low-molecular-weight Gd-DTPA because of its poor cancer tropism and difficulty to reach effective doses in tumor tissues (Figure 4). Several benefits have been achieved by incorporating Gd-DTPA in hybrid CaP nanocarriers in this study. First, it has dramatically optimized the pharmacokinetics of Gd-DTPA resulting in high accumulation in solid tumors, which could further highly selectively enhance the contrast of cancerous tissues due to their increased molecular relaxivity and provide a much higher dose of Gd-chelates for operational cancer NCT. Moreover, the targeted delivery of Gd-DTPA to tumors with high tumor-to-blood ratio decreased the risk of damage to normal tissues. Moreover, the precise size control of Gd-DTPA/CaP is important for broad delivery into tumor tissues, as nanocarriers of sub-100 nm size were demonstrated to deeply penetrate the tumor tissues.[38] Consequently, through Gd-DTPA/CaP, we realized our concept of nanocarriers incorporating Gd-chelates for MR imaging-guided local thermal neutron irradiation directed to effective cancer treatment.

The safety of Gd-DTPA/CaP is also an important factor for further biological applications and clinical translation. Gd-DTPA/CaP appear to be well tolerated, as no significant decrease in cell viability was observed after exposure for 24 h (Figure 3), and the *in vivo* experiments did not show any severe side effects. In the clinical stage, Gd-DTPA has demonstrated low toxicity and good renal tolerance in healthy individuals[39] as well as in patients with moderate levels of underlying kidney disease,[40] only rare cases of nephrogenic systemic fibrosis (NSF) have been reported in patients with advanced kidney diseases, such as end-stage renal disease (ESRD).[41,42] Nevertheless, as NSF could be avoided by administrating low doses of Gd-based agents,[43] the incorporation of such compounds in nanocarriers could provide safe strategies for GdNCT in clinical applications by allowing for the injection of much lower doses due to their tumor targeting ability.

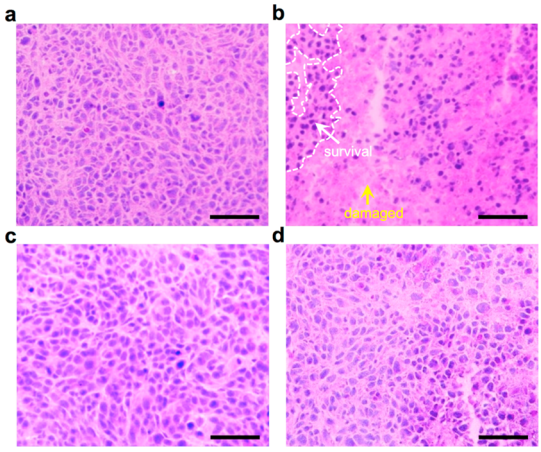

Figure 6. H&E staining of subcutaneous C26 tumors after neutron capture therapy. (a) Tumor treated with Gd-DTPA/CaP but without thermal neutron irradiation. (b) Tumor treated with Gd-DTPA/CaP and thermal neutron irradiation for 1 h. The GdNCT damaged most cancer cells, and only a few of them remained. (c) Tumor treated with Gd-DTPA but without thermal neutron irradiation. (d) Tumor treated with Gd-DTPA and thermal neutron irradiation for 1 h. Scale bar 50 μm.

For instance, the dose of Gd-DTPA/CaP used in this study is much lower than that used for Gd-DTPA-based MRI contrast enhancement in clinical uses.

CONCLUSION

In summary, we have presented a strategy for incorporating low-molecular-weight Gd(III) chelates inside CaP micelles for dual noninvasive MR cancer diagnosis and NCT, without the necessity of loading individual contrast and therapeutic drugs, which is usually required in theranostics. The PEGylated Gd-DTPA/CaP micelles featured with high r_1 relaxivity could sensitively enhance contrast of neoplastic tissues for MR imaging-guided tumor positioning. The micelles also had high therapeutic efficacy for GdNCT against solid tumors, as the high accumulation of the micelle-delivered Gd-DTPA in tumor tissues could effectively damage cancer cells by γ-rays or electron emission from the Gd nuclides. Gd-DTPA/CaP significantly improved the pharmacological properties of Gd-DTPA, such as plasma clearance, tumor accumulation, contrast specificity, and antitumor effects in GdNCT, demonstrating a potential for further biomedical applications. This study broadened the applications of CaP micelles to radiotherapy and provided a strategy for designing and developing nanocarriers for imaging-guided NCT of tumors.

MATERIALS AND METHODS

Materials and Animals. α-Methoxy-ω-aminopoly(ethylene glycol) (PEG-NH_2; M_W = 12 000) was bought from NOF Co., Inc. (Tokyo, Japan). β-Benzyl-L-aspartate *N*-carboxy-anhydride (BLA-NCA) was bought from Chuo Kaseihin Co., Inc. (Tokyo, Japan). $CaCl_2$, NaCl, $NaHPO_4$, NaOH, *N*,*N*-dimethylformamide (DMF) and dichloromethane (CH_2Cl_2) were bought from Wako Pure Chemical Industries, Ltd. (Osaka, Japan). DMF and CH_2Cl_2 were purified by distillation under reduced pressure. 2-(4-(2-Hydroxyethyl)-1-piperazinyl)ethanesulfonic acid (HEPES) was bought from Dojindo Molecular Technologies, Inc. (Kumamoto, Japan). Tris base,

fetal bovine serum (FBS), Gd-DTPA, and Dulbecco's modified Eagle medium (DMEM) were obtained from Sigma-Aldrich (St. Louis, Missouri), including the Gd-DTPA was converted to its sodium salt by adjusting to pH 7 with NaOH and was lyophilized before use. Murine colon adenocarcinoma 26 (C26) cells were kindly supplied by the National Cancer Center (Tokyo, Japan) and cultured with DMEM containing 10% FBS in a humidified atmosphere containing 5% CO_2 at 37 °C. BALB/c mice (female, 6 weeks, 18−20 g) were purchased from Charles River Laboratories, Inc. (Tokyo, Japan), and all animal experiments were carried out following the policies of the Animal Ethics Committee of the University of Tokyo.

Synthesis of PEG−PAsp Block Copolymer. First, PEG-poly(β-benzyl-L-aspartate) (PEG−PBLA) was synthesized through the ring-opening polymerization of BLA-NCA, as previously described.[44] Briefly, BLA-NCA (0.98 g, 4 mmol) was dissolved in a mixture of DMF (2 mL) and CH_2Cl_2 (18 mL) and initiated for polymerization by the addition of PEG-NH_2 (1.2 g, 0.1 mmol) dissolved in DMF and CH_2Cl_2. The polymerization reaction was carried out at 35 °C for 72 h under the protection of argon gas. The PEG−PBLA was obtained after precipitating the reaction solution in diethyl ether and drying under a vacuum. The degree of polymerization (DP) of PBLA was determined to be 40 by ^{1}H NMR after comparing the proton peak ratio of the methylene units of PEG ((−$C\underline{H}_2C\underline{H}_2$O−): δ = 3.7 ppm) with the phenyl groups of PBLA (−$C_6\underline{H}_5$: δ = 7.3 ppm) in the ^{1}H NMR spectrum. Then, PEG−PBLA (1 g) was dissolved in acetonitrile (20 mL), followed by the addition of 0.5 M NaOH (20 mL) and stirring at room temperature. After 1.5 h, the reaction mixture was dialyzed (MWCO: 3.5 kDa) against Milli-Q water. Finally, the solution inside the dialysis bag was lyophilized to obtain PEG−PAsp with 40DP of PAsp.

Preparation of Gd-DTPA/CaP Micelles. The Gd-DTPA/CaP polymeric micelles were prepared according to a previously described method.[29] Briefly, 1 mL of Tris-HCl buffer (pH 7.6) containing 250 mM $CaCl_2$ was mixed with 1 mL of 50 mM HEPES saline buffer (NaCl 140 mM, pH 7.1) containing Na_2HPO_4 (6 mM), Gd-DTPA (2 mM), and PEG−PAsp (5 mM based on carboxylic acid groups) to yield the Gd-DTPA/CaP polymeric micelles. Then, the obtained Gd-DTPA/CaP micelles were subjected to hydrothermal treatment at 120 °C for 20 min under a pressure of 100 kPa. After the hydrothermal treatment, the Gd-DTPA/CaP micelles were purified by dialysis and ultrafiltration with 25 mM HEPES saline buffer at pH 7.4 containing 140 mM NaCl and 2 mM $CaCl_2$ to mimic the biological conditions.

Characterization of Gd-DTPA/CaP. The average diameter of the Gd-DTPA/CaP micelles was measured by dynamic light scattering (DLS) using a (Zetasizer Nano ZS90, Malvern Instruments, UK), while the concentration of Gd-DTPA was determined by Inductively coupled plasma mass spectrometry (ICP-MS) (4500 ICP-MS, Hewlett-Packard, Delaware, USA). The morphology of the Gd-DTPA/CaP micelles was investigated using a MMAFM, Nanoscope V (Bruker AXS, Madison, USA) under the ScabAsyst Atomic Force Microscopy Imaging mode with silicon probes. The longitudinal relaxation time T_1 (s) of Gd-DTPA/CaP at different concentration of Gd-DTPA (0.1, 0.2, 0.3, 0.4, and 0.5 mM) was measured by a ^{1}H NMR analyzer (JNM-MU25A, JEOL, Tokyo, Japan) using the inversion−recovery pulse sequence method at 0.59 T and 37 °C. This measurement was conducted in 10 mM PBS buffer (NaCl 140 mM) at pH 6.7 to mimic the physicochemical conditions of tumors. Then, the r_1 relaxivities of Gd-DTPA/CaP and Gd-DTPA were calculated using the following equation:

$$r_1 = (1/T_1 - 1/T_{1(0)})/[Gd]$$

Where [*Gd*] represents the concentration of Gd-DTPA (mM), $1/T_{1(0)}$ (s^{-1}) is the relaxation rate without paramagnetic species, and $1/T_1$ (s^{-1}) is the relaxation rate with paramagnetic species. The release profile of Gd-DTPA from the CaP nanoparticles was conducted by dialysis (MWCO = 6 kDa−8 kDa): 1 mL of Gd-DTPA/CaP was diluted against 99 mL of DMEM medium containing 10% FBS that was adjusted to the pH level of tumor tissues (pH 6.7) using HCl and then incubated at 37 °C with continuous shaking to mimic the physiological conditions. Finally, 100 μL of the medium outside the dialysis bag was collected at defined time intervals and measured by ICP-MS after dilution with 1% HNO_3. The relaxivity and the Gd-DTPA release at pH 7.4 were measured as well as that of the control.

***In Vitro* Toxicity of Gd-DTPA/CaP.** C26 cells were seeded in 96-well plates at a cell concentration of 3.5 × 10^3 cells per well and incubated for 24 h. Then, Gd-DTPA or Gd-DTPA/CaP was added to each well to achieve a concentration of 100 μM based on Gd-DTPA, and 24 h later, the plates were irradiated with a neutron beam at a rate of 1.6−2.2 × 10^{12} neutron/mm^2 for 1 h. The irradiated cells were incubated for another 24 h. Then, the availability was tested with the addition of a Cell Counting Kit-8 (CCK-8) (Dojindo Molecular Technologies, Inc., Japan), and finally the cells were counted with a microplate reader (Model 680, Bio-Rad Laboratories, Inc., Hercules, US) at 450 nm. The availability of the C26 cells that were exposed to Gd-DTPA or Gd-DTPA/CaP for 48 h without irradiation was tested as control.

***In Vivo* Pharmacokinetics Study of Gd-DTPA/CaP.** The subcutaneous C26 tumor models were prepared by subcutaneously inoculating 100 μL of C26 tumor cells into BALB/c mice at a concentration of 1 × 10^6 cell/mL. Then, an equal dose of 0.02 mmol/kg based on Gd-DTPA of Gd-DTPA/CaP or Gd-DTPA was intravenously injected to the C26 tumor-bearing mice until the tumor volume reached 100 mm^3. Thereafter, the mice were sacrificed, and the blood was collected from the inferior vena cava with a syringe, heparinized, and centrifuged to obtain plasma, while the tumor tissues and main organs were excised at 3, 6, 10, and 24 h after injection. The plasma, tumor tissues, and organs were dissolved with 90% HNO_3, dried by evaporation, and resuspended with 1% HNO_3 for the ICP-MS measurements to determine the Gd concentration.

***In Vivo* MRI Measurements.** For *in vivo* MR cancer imaging, subcutaneous tumors were prepared by the subcutaneous injection of C26 cells to BALB/c mice, and MRI measurements were conducted with 1T MRI equipment until the tumor volume reached approximately 100 mm^3. The subcutaneous C26 tumor-bearing mice were intravenously injected with Gd-DTPA/CaP at a dose of 0.05 mmol/kg based on Gd-DTPA for MRI detection, using Gd-DTPA (0.22 mmol/kg) as control. *In vivo* T_1-weighted MR imaging parameters: spin−echo method, repetition time (TR) = 400 ms, echo time (TE) = 11 ms, field of view (FOV) = 48 × 48 mm, matrix size = 256 × 256, and slice thickness = 2 mm. The contrast intensity of the region of interest (ROI) in the tumor and normal regions (muscle) were measured by the software and compared after normalization.

***In Vivo* GdNCT of Solid Tumors with Gd-DTPA/CaP.** The subcutaneous C26 tumor-bearing BALB/c mice were intravenously injected with 0.2 mL of Gd-DTPA/CaP or Gd-DTPA at a dose of 8.25 mg/kg based on Gd-compound. Twenty-four hours later, the mice were locally irradiated with a thermal neutron beam for 1 h at a rate of 1.6−2.2 × 10^{12} neutron/cm^2 at the Kyoto University Research Reactor (KUR). The tumor size was measured before and after irradiation, and the volume (*V*) was calculated using the following equation:

$$V = (a \times b^2)/2$$

where (*a*) and (*b*) are the major and minor axes of the tumor measured by a caliper. The subcutaneous C26 tumor-bearing BALB/c mice were administered with Gd-DTPA/CaP or Gd-DTPA at the same dose but were not subjected to thermal neutron irradiation as control. The body weight of each mouse was measured as an indicator of systemic toxicity.

Pathological Investigation of Tumor Tissues after GdNCT. After the *in vivo* GdNCT experiments, the tumor tissues were harvested, embedded in OCT compound, and frozen with acetone/dry ice mixture. Thereafter, the samples were sliced to 4-μm thickness with a cryostat (CM1950, Leica, Germany), fixed with 4% paraformaldehyde (PFA) solution in PBS buffer, and finally stained with hematoxylin and eosin (H&E). The images of the stained tumor slices were characterized using an AX80 microscope (Olympus, Japan).

Statistical Analysis. Data in the manuscript were expressed as the mean and SD, and the significance of the results was analyzed by Student's *t*-test. *p*-values lower than 0.05 were considered statistically significant.

Conflict of Interest: The authors declare no competing financial interest.

Acknowledgment. This research was financially supported by the Center of Innovation Program (COI stream from Japan Science and Technology Agency (JST) and Funding Program for World-Leading Innovative R&D on Science and Technology (FIRST) from the Japan Society for the Promotion of Science (JSPS) (K.K.). This work was also partially supported by a Grant-in-Aid for Exploratory Research, JSPS (N.N.). P.M. thanks the support of a JSPS fellowship (P13042). TEM measurements were conducted at the Research Hub for Advanced Nano Characterization, The University of Tokyo, supported by the Ministry of Education, Culture, Sports, Science and Technology (MEXT), Japan. We thank Ms. Y. Sakurai (UT), Ms. S. Shibata and Ms. A. Sekita (NIRS) for technical support.

Supporting Information Available: The biodistribution of Gd-DTPA/CaP and Gd-DTPA in main organs. The Supporting Information is available free of charge on the ACS Publications website at DOI: 10.1021/acsnano.5b00532.

REFERENCES AND NOTES

1. Barth, R. F.; Vicente, M. G. H.; Harling, O. K.; Kiger, W. S.; Riley, K. J.; Binns, P. J.; Wagner, F. M.; Suzuki, M.; Aihara, T.; Kato, I.; *et al.* Current Status of Boron Neutron Capture Therapy of High Grade Gliomas and Recurrent Head and Neck Cancer. *Radiat. Oncol.* **2012**, *7*, 146–166.
2. Moss, R. L. Critical Review, with an Optimistic Outlook, on Boron Neutron Capture Therapy (BNCT). *Int. J. Appl. Radiat. Isot.* **2014**, *88*, 2–11.
3. Yanagie, H.; Tomita, T.; Kobayashi, H.; Fujii, Y.; Takahashi, T.; Hasumi, K.; Nariuchi, H.; Sekiguchi, M. Application of Boronated Anti-CEA Immunoliposome to Tumour Cell Growth Inhibition in *in Vitro* Boron Neutron Capture Therapy Model. *Br. J. Cancer* **1991**, *63*, 522–526.
4. Kueffer, P. J.; Maitz, C. A.; Khan, A. A.; Schuster, S. A.; Shlyakhtina, N. I.; Jalisatgi, S. S.; Brockman, J. D.; Nigg, D. W.; Hawthorne, M. F. Boron Neutron Capture Therapy Demonstrated in Mice Bearing EMT6 Tumors Following Selective Delivery of Boron by Rationally Designed Liposomes. *Proc. Natl. Acad. Sci. U. S. A.* **2013**, *110*, 6512–6517.
5. Weissleder, R.; Pittet, M. J. Imaging in the Era of Molecular Oncology. *Nature* **2008**, *452*, 580–589.
6. Cabral, H.; Nishiyama, N.; Kataoka, K. Supramolecular Nanodevices: From Design Validation to Theranostic Nanomedicine. *Acc. Chem. Res.* **2011**, *44*, 999–1008.
7. Yanagie, H.; Ogata, A.; Sugiyama, H.; Eriguchi, M.; Takamoto, S.; Takahashi, H. Application of Drug Delivery System to Boron Neutron Capture Therapy for Cancer. *Expert Opin. Drug Delivery* **2008**, *5*, 427–443.
8. Sharma, P.; Brown, S. C.; Walter, G.; Santra, S.; Scott, E.; Ichikawa, H.; Fukumori, Y.; Moudgil, B. M. Gd Nanoparticulates: from Magnetic Resonance Imaging to Neutron Capture Therapy. *Adv. Powder Technol.* **2007**, *18*, 663–698.
9. Coderre, J. A.; Morris, G. M. The Radiation Biology of Boron Neutron Capture Therapy. *Radiat. Res.* **1999**, *151*, 1–18.
10. Martin, R. F.; Dcunha, G.; Pardee, M.; Allen, B. J. Induction of Double-Strand Breaks Following Neutron-Capture by DNA-Bound Gd-157. *Int. J. Radiat. Biol.* **1988**, *54*, 205–208.
11. De Stasio, C.; Casalbore, P.; Pallini, R.; Gilbert, B.; Sanita, F.; Ciotti, M. T.; Rosi, G.; Festinesi, A.; Larocca, L. M.; Rinelli, A.; *et al.* Gadolinium in Human Glioblastoma Cells for Gadolinium Neutron Capture Therapy. *Cancer Res.* **2001**, *61*, 4272–4277.
12. Weinmann, H. J.; Brasch, R. C.; Press, W. R.; Wesbey, G. E. Characteristics of Gadolinium-DTPA Complex: A Potential NMR Contrast Agent. *AJR, Am. J. Roentgenol.* **1984**, *142*, 619–624.
13. Kataoka, K.; Harada, A.; Nagasaki, Y. Block Copolymer Micelles for Drug Delivery: Design, Characterization and Biological Significance. *Adv. Drug Delivery Rev.* **2001**, *47*, 113–131.
14. Perry, J. L.; Herlihy, K. P.; Napier, M. E.; Desimone, J. M. PRINT: A Novel Platform Toward Shape and Size Specific Nanoparticle Theranostics. *Acc. Chem. Res.* **2011**, *44*, 990–998.
15. Nishiyama, N.; Kataoka, K. Current State, Achievements, and Future Prospects of Polymeric Micelles as Nanocarriers for Drug and Gene Delivery. *Pharmacol. Ther.* **2006**, *112*, 630–648.
16. Peer, D.; Karp, J. M.; Hong, S.; Farokhzad, O. C.; Margalit, R.; Langer, R. Nanocarriers as an Emerging Platform for Cancer Therapy. *Nat. Nanotechnol.* **2007**, *2*, 751–760.
17. Torchilin, V. P. PEG-Based Micelles as Carriers of Contrast Agents for Different Imaging Modalities. *Adv. Drug Delivery Rev.* **2002**, *54*, 235–252.
18. Kaida, S.; Cabral, H.; Kumagai, M.; Kishimura, A.; Terada, Y.; Sekino, M.; Aoki, I.; Nishiyama, N.; Tani, T.; Kataoka, K. Visible Drug Delivery by Supramolecular Nanocarriers Directing to Single-Platformed Diagnosis and Therapy of Pancreatic Tumor Model. *Cancer Res.* **2010**, *70*, 7031–7041.
19. Mi, P.; Cabral, H.; Kokuryo, D.; Rafi, M.; Terada, Y.; Aoki, I.; Saga, T.; Ishii, T.; Nishiyama, N.; Kataoka, K. Gd-DTPA-Loaded Polymer-Metal Complex Micelles with High Relaxivity for MR Cancer Imaging. *Biomaterials* **2013**, *34*, 492–500.
20. Hwang, K. C.; Lai, P. D.; Chiang, C. S.; Wang, P. J.; Yuan, C. J. Neutron Capture Nuclei-Containing Carbon Nanoparticles for Destruction of Cancer Cells. *Biomaterials* **2010**, *31*, 8419–8425.
21. Geninatti-Crich, S.; Alberti, D.; Szabo, I.; Deagostino, A.; Toppino, A.; Barge, A.; Ballarini, F.; Bortolussi, S.; Bruschi, P.; Protti, N.; *et al.* MRI-Guided Neutron Capture Therapy by Use of a Dual Gadolinium/Boron Agent Targeted at Tumour Cells through Upregulated Low-Density Lipoprotein Transporters. *Chem. Eur. J.* **2011**, *17*, 8479–8486.
22. Feakes, D. A.; Shelly, K.; Knobler, C. B.; Hawthorne, M. F. $Na_3[B_{20}H_{17}NH_3]$: Synthesis and Liposomal Delivery to Murine Tumors. *Proc. Natl. Acad. Sci. U. S. A.* **1994**, *91*, 3029–3033.
23. Bridot, J. L.; Dayde, D.; Riviere, C.; Mandon, C.; Billotey, C.; Lerondel, S.; Sabattier, R.; Cartron, G.; Le Pape, A.; Blondiaux, G.; *et al.* Hybrid Gadolinium Oxide Nanoparticles Combining Imaging and Therapy. *J. Mater. Chem.* **2009**, *19*, 2328–2335.
24. Tachikawa, S.; Miyoshi, T.; Koganei, H.; El-Zaria, M. E.; Vinas, C.; Suzuki, M.; Ono, K.; Nakamura, H. Spermidinium Closo-Dodecaborate-Encapsulating Liposomes as Efficient Boron Delivery Vehicles for Neutron Capture Therapy. *Chem. Commun.* **2014**, *50*, 12325–12328.
25. Yinghuai, Z.; Peng, A. T.; Carpenter, K.; Maguire, J. A.; Hosmane, N. S.; Takagaki, M. Substituted Carborane-Appended Water-Soluble Single-Wall Carbon nanotubes: New Approach to Boron Neutron Capture Therapy Drug Delivery. *J. Am. Chem. Soc.* **2005**, *127*, 9875–9880.
26. Matsumura, Y.; Maeda, H. A New Concept for Macromolecular Therapeutics in Cancer Chemotherapy: Mechanism of Tumoritropic Accumulation of Proteins and the Antitumor Agent Smancs. *Cancer Res.* **1986**, *46*, 6387–6392.
27. Kakizawa, Y.; Miyata, K.; Furukawa, S.; Kataoka, K. Size-Controlled Formation of a Calcium Phosphate-Based Organic-Inorganic Hybrid Vector for Gene Delivery Using Poly(Ethylene Glycol)-Block-Poly(Aspartic Acid). *Adv. Mater.* **2004**, *16*, 699–702.
28. Kakizawa, Y.; Kataoka, K. Block Copolymer Self-Assembly into Monodispersive Nanoparticles with Hybrid Core of Antisense DNA and Calcium Phosphate. *Langmuir* **2002**, *18*, 4539–4543.
29. Mi, P.; Kokuryo, D.; Cabral, H.; Kumagai, M.; Nomoto, T.; Aoki, I.; Terada, Y.; Kishimura, A.; Nishiyama, N.; Kataoka, K. Hydrothermally Synthesized PEGylated Calcium Phosphate Nanoparticles Incorporating Gd-DTPA for Contrast Enhanced MRI Diagnosis of Solid Tumors. *J. Controlled Release* **2014**, *174*, 63–71.
30. Tannock, I. F.; Rotin, D. Acid pH in Tumors and Its Potential for Therapeutic Exploitation. *Cancer Res.* **1989**, *49*, 4373–4384.
31. LeGeros, R. Z. Biodegradation and Bioresorption of Calcium Phosphate Ceramics. *Clin. Mater.* **1993**, *14*, 65–88.
32. Zhang, M.; Ishii, A.; Nishiyama, N.; Matsumoto, S.; Ishii, T.; Yamasaki, Y.; Kataoka, K. PEGylated Calcium Phosphate

Nanocomposites as Smart Environment-Sensitive Carriers for siRNA Delivery. *Adv. Mater.* **2009**, *21*, 1–6.
33. Kakizawa, Y.; Furukawa, S.; Kataoka, K. Block Copolymer-Coated Calcium Phosphate Nanoparticles Sensing Intracellular Environment for Oligodeoxynucleotide and siRNA Delivery. *J. Controlled Release* **2004**, *97*, 345–356.
34. Caravan, P.; Ellison, J. J.; McMurry, T. J.; Lauffer, R. B. Gadolinium(III) Chelates as MRI Contrast Agents: Structure, Dynamics, and Applications. *Chem. Rev.* **1999**, *99*, 2293–2352.
35. Terreno, E.; Castelli, D. D.; Viale, A.; Aime, S. Challenges for Molecular Magnetic Resonance Imaging. *Chem. Rev.* **2010**, *110*, 3019–3042.
36. De Stasio, G.; Rajesh, D.; Casalbore, P.; Daniels, M. J.; Erhardt, R. J.; Frazer, B. H.; Wiese, L. M.; Richter, K. L.; Sonderegger, B. R.; Gilbert, B.; *et al.* Are Gadolinium Contrast Agents Suitable for Gadolinium Neutron Capture Therapy? *Neurol. Res.* **2005**, *27*, 387–398.
37. Soloway, A. H.; Tjarks, W.; Barnum, B. A.; Rong, F. G.; Barth, R. F.; Codogni, I. M.; Wilson, J. G. The Chemistry of Neutron Capture Therapy. *Chem. Rev.* **1998**, *98*, 1515–1562.
38. Cabral, H.; Matsumoto, Y.; Mizuno, K.; Chen, Q.; Murakami, M.; Kimura, M.; Terada, Y.; Kano, M. R.; Miyazono, K.; Uesaka, M.; *et al.* Accumulation of Sub-100 nm Polymeric Micelles in Poorly Permeable Tumours Depends on Size. *Nat. Nanotechnol.* **2011**, *6*, 815–823.
39. Carr, D. H.; Brown, J.; Bydder, G. M.; Steiner, R. E.; Weinmann, H. J.; Speck, U.; Hall, A. S.; Young, I. R. Gadolinium-DTPA as a Contrast Agent in MRI: Initial Clinical-Experience in 20 Patients. *AJR, Am. J. Roentgenol.* **1984**, *143*, 215–224.
40. Niendorf, H. P.; Haustein, J.; Cornelius, I.; Alhassan, A.; Clauss, W. Safety of Gadolinium-DTPA: Extended Clinical Experience. *Magn. Reson. Med.* **1991**, *22*, 222–228.
41. Grobner, T. Gadolinium-A Specific Trigger for the Development of Nephrogenic Fibrosing Dermopathy and Nephrogenic Systemic Fibrosis? *Nephrol., Dial., Transplant.* **2006**, *21*, 1745–1745.
42. Deo, A.; Fogel, M.; Cowper, S. E. Nephrogenic Systemic Fibrosis: A Population Study Examining the Relationship of Disease Development to Gadolinium Exposure. *Clin. J. Am. Soc. Nephrol.* **2007**, *2*, 264–267.
43. Perazella, M. A. Current Status of Gadolinium Toxicity in Patients with Kidney Disease. *Clin J. Am. Soc. Nephrol.* **2009**, *4*, 866–866.
44. Koide, A.; Kishimura, A.; Osada, K.; Jang, W. D.; Yamasaki, Y.; Kataoka, K. Semipermeable Polymer Vesicle (PICsome) Self-Assembled in Aqueous Medium from a Pair of Oppositely Charged Block Copolymers: Physiologically Stable Micro-/Nanocontainers of Water-Soluble Macromolecules. *J. Am. Chem. Soc.* **2006**, *128*, 5988–5989.